Simultaneous Trajectory Tracking Control of Position and Force with Pneumatic Cylinder Driving Apparatus

Ji-Seong Jang*

Division of Mechanical Engineering, Pukyong National University, San 100, Yongdang-Dong, Nam-Gu, Busan 608-739, Republic of Korea

In this study, a position and force simultaneous trajectory tracking control algorithm is proposed for a driving apparatus that consists of two pneumatic cylinders connected in series. The controller applied to the driving apparatus is composed of a non-interaction controller to compensate for interaction between cylinders and a disturbance observer aimed to reduce the effect of model discrepancy that cannot be compensated by the non-interaction controller. The effectiveness of the proposed control algorithm is proved by experimental results.

Key Words : Compressibility, Low Stiffness, Pneumatic Cylinder, Position and Force Trajectory Tracking

1. Introduction

Pneumatic cylinder driving apparatus are widely used in industrial applications owing to the easy installation and maintenance. However, the most common application of the pneumatic cylinder driving apparatus is a simply repeating operation (Johira, 1997 ; McGuirk et al., 1998) because it is not easy to obtain high performance control results due to several nonlinear characteristics of the air and cylinder such as compressibility, low damping characteristics and lower driving force compared to the friction force. Therefore, to apply a pneumatic cylinder driving apparatus to a new field, an application which makes the best use of the pneumatic cylinder should be selected and the controller compensating the nonlinear characteristics should be designed. The position trajectory tracking performance of a pneumatic cylinder driving apparatus is inferior to the others because of the low stiffness characteristics but it means that the interaction between the pneumatic cylinders is smaller than the others (Noritugu, 1993). So, the low stiffness characteristics has a merit in case that multiple cylinders are driven at the same time and each cylinder has a different output.

Yamafuji and Fukushima (1988) used LQ controller for simultaneous control of position and force with a pneumatic cylinder, but they applied the controller only to step input because force control was not started until the position error was reached within a certain limit.

The goal of this paper is to design a simultaneous trajectory tracking controller of position and force for a driving apparatus composed of two pneumatic cylinders connected in serious and two proportional flow control valves to control each cylinder. The controller applied to the driving apparatus is composed of a non-interaction controller and a disturbance observer. The non-interaction controller to compensate interaction between two cylinders is designed based on the dominating equations of the driving apparatus. The disturbance observer using a control system with the non-interaction controller as an internal model is designed to reduce the effect of modeling error that cannot be compensated by the non-interaction controller.

* **E-mail** : jangjs@pknu.ac.kr
TEL : +82-51-620-1583; **FAX** : +82-51-620-1574
Division of Mechanical Engineering, Pukyong National University, San 100, Yongdang-Dong, Nam-Gu, Busan 608-739, Republic of Korea. (Manuscript **Received** September 23, 2004; **Revised** March 19, 2005)

The performance of the proposed control algorithm is evaluated by experiments and the experimental results show that the pneumatic cylinder driving apparatus with the proposed control algorithm tracks the given position and force reference inputs accurately.

2. Configuration of the Driving Apparatus

Figure 1 shows the configuration of the driving apparatus. It is primarily composed of two pneumatic cylinders, a personal computer, 12-bit A/D and D/A converter, and two control valves. The pneumatic cylinders (①, ③ CA1B30-300 : SMC Corporation) are single rod type whose inside diameter is 40 mm, rod diameter is 12 mm and the stroke is 300 mm. The control valves (⑤ MPYE-5-1/8HF-010B, ⑥ MPYE-5-1/4LF-010B : FESTO Corporation) are proportional flow control valves. The position measurement is carried out by a linear potentiometer (④ LTM300S : GEFRAN Corporation) and the force is measured by load cell (② MNT-100L : CAS Corporation)

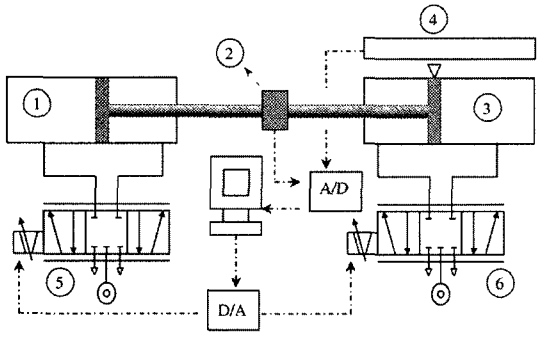

① Cylinder for force control ② Load cell
③ Cylinder for position control ④ Potentiometer
⑤⑥ Proportional flow control valve

Fig. 1 Configuration of the pneumatic cylinder driving apparatus

3. Modeling

3.1 Dominating equations

Figure 2 shows the schematic representation of the pneumatic cylinder driving apparatus.

In Fig. 2, A [m^2] is the pressurized area of piston, F [N] is the force, G [kg/s] is the mass flow rate, L [m] is the cylinder full stroke, M [kg] is mass of the piston and rod, P [Pa] is the absolute pressure, T [K] is the absolute temperature, V [m^3] is the control volume, x [m] is the displacement, subscript 1, 2 mean the incoming side and the outgoing side respectively, subscript a, b mean the force control side and the position control side respectively.

Eqs. (1) ~ (4) describe the dynamic pressure change in the cylinder chambers. Here it is assumed that air is a perfect gas, pressure and temperature within the chamber are homogeneous and the process is adiabatic.

$$\frac{dP_{a1}}{dt}=\frac{\kappa}{V_{a1}}\left\{P_{a1}A_1\frac{dx}{dt}+G_{a1}RT_{a1}\right\} \quad (1)$$

$$\frac{dP_{a2}}{dt}=\frac{\kappa}{V_{a2}}\left\{-P_{a2}A_2\frac{dx}{dt}-G_{a2}RT_{a2}\right\} \quad (2)$$

$$\frac{dP_{b1}}{dt}=\frac{\kappa}{V_{b1}}\left\{-P_{b1}A_1\frac{dx}{dt}+G_{b1}RT_{b1}\right\} \quad (3)$$

$$\frac{dP_{b2}}{dt}=\frac{\kappa}{V_{b2}}\left\{P_{b2}A_2\frac{dx}{dt}-G_{b2}RT_{b2}\right\} \quad (4)$$

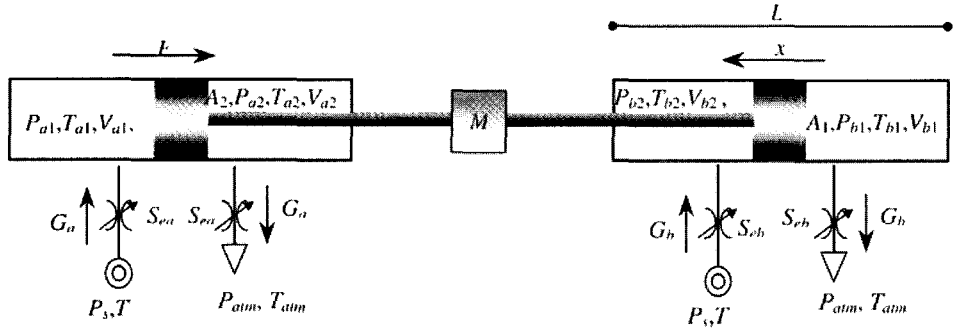

Fig. 2 Schematic diagram of the driving apparatus

In Eqs. (1)~(4), κ is the specific heat ratio.

Eqs. (5) and (6) show dynamic equation and output force respectively.

$$M\frac{d^2x}{dt^2}=A_1P_{b1}-A_2P_{b2}-A_1P_{a1}+A_2P_{a2} -B\frac{dx}{dt}-F_c\,\mathrm{sgn}\left(\frac{dx}{dt}\right) \tag{5}$$

$$F=A_1P_{a1}-A_2P_{a2}+A_1P_{b1}-A_2P_{b2} \tag{6}$$

In Eq. (5), B [N/(m/s)] is the dynamic friction coefficient, F_c [N] is the friction force.

3.2 Linearization

The linearized equations of the mass flow passing the control valves (Merritt, 1967) become

$$G_{a1}=k_{qa}u_a-k_{p0}P_{a1} \tag{7}$$

$$G_{a2}=k_{qa}u_a+k_{p0}P_{a2} \tag{8}$$

$$G_{b1}=k_{qb}u_b-k_{p0}P_{b1} \tag{9}$$

$$G_{b2}=k_{qb}u_b+k_{p0}P_{b2} \tag{10}$$

where k_q [(kg/s)/V] is the flow gain of the control valve, k_b [(kg/s)/Pa] is the flow-pressure coefficient of the control valve, and u [V] is the control input. In Eqs. (7)~(10), k_{pa} and k_{pb} were expressed as k_{p0} because there was little difference between k_{pa} and k_{pb}.

At an operating point $x=x_0$, $P_{a1}=P_{b1}=P_{10}$, $P_{a2}=P_{b2}=P_{20}$, $V_{a1}=V_{a2}=V_{b1}=V_{b2}=V_0$, and $T_{a1}=T_{a2}=T_{b1}=T_{b2}=T_{atm}$, the linear model of the driving apparatus can be obtained as follows.

$$\begin{bmatrix}F(s)\\x(s)\end{bmatrix}=H(s)\begin{bmatrix}u_a(s)\\u_b(s)\end{bmatrix},\quad H(s)=\begin{bmatrix}H_{aa}(s) & H_{ab}(s)\\-H_{ba}(s) & H_{bb}(s)\end{bmatrix}$$

$$H_{aa}(s)=\frac{H_{aan}(s)}{H_{aad}(s)},\quad H_{ab}(s)=\frac{H_{abn}(s)}{H_{abd}(s)}$$

$$H_{ba}(s)=\frac{H_{ban}(s)}{H_{bad}(s)},\quad H_{bb}(s)=\frac{H_{bbn}(s)}{H_{bbd}(s)}$$

$$\begin{aligned}&H_{aan}(s)=H_{ban}(s)=\eta k_{qa}(A_1+A_2)\\&H_{abn}(s)=H_{bbn}(s)=\eta k_{qb}(A_1+A_2)\\&H_{aad}(s)=H_{abd}(s)=s+\eta k_{p0}\\&H_{bad}(s)=H_{bbd}(s)=Ms^3+(\eta k_{p0}M+B)s^2\\&\qquad+(\eta k_{p0}B+2K_E)s\end{aligned} \tag{11}$$

$$\eta=\frac{\kappa RT_{atm}}{V_0},\quad K_E=A_1^2\frac{\kappa P_{10}}{V_0}+A_2^2\frac{\kappa P_{20}}{V_0}$$

4. Controller Design

4.1 Non-interaction controller design

From the Eq. (11), the relationship between two control inputs, $u_a(s)$, $u_b(s)$ and two outputs, $F(s)$, $x(s)$, can be represented by

$$F(s)=H_{aa}(s)\,u_a(s)+H_{ab}(s)\,u_b(s) \tag{12}$$

$$x(s)=-H_{ba}(s)\,u_a(s)+H_{bb}(s)\,u_b(s) \tag{13}$$

and it can be known that the driving apparatus exhibits the property of interaction between control inputs and outputs. Therefore, to control each output to a desired value, controller that can compensate the interaction effects have to be designed.

Fig. 3 shows a block diagram of a unity feedback control system.

Where $R(s)$ is $[F_r(s)x_r(s)]^T$ and $Y(s)$ is $[F(s)x(s)]^T$.

In Fig. 3, all realizable stabilizing controllers $C_n(s)$ derived from Youla parametrization (Desoer, 1980; Umeno and Hori, 1989) are given by

$$\begin{aligned}C_n(s)&=Q(H(s))\\&=(\tilde{W}_H(s)+D_H(s)Q(s))(\tilde{Z}_H(s)-N_H(s)Q(s))^{-1}\end{aligned} \tag{14}$$

where $D_H(s)$ and $N_H(s)$ are the denominator and numerator of right coprime fraction of $H(s)$, and $\tilde{W}_H(s)$, $\tilde{Z}_H(s)$ are matrices that satisfy the Bezout identity described in Eq. (15).

$$\tilde{N}_H(s)\,\tilde{W}_H(s)+\tilde{D}_H(s)\,\tilde{Z}_H(s)=I \tag{15}$$

where $\tilde{D}_H(s)$ and $\tilde{N}_H(s)$ are denominator and numerator of left coprime fraction of $H(s)$. One of matrices satisfying Eq. (15) can be obtained as follows.

$$\begin{aligned}&H(s)\in RH_\infty,\ N_H(s)=\tilde{N}_H(s)=H(s)\\&D_H(s)=\tilde{D}_H(s)=I,\ \tilde{W}_H(s)=0,\ \tilde{Z}_H(s)=I\end{aligned} \tag{16}$$

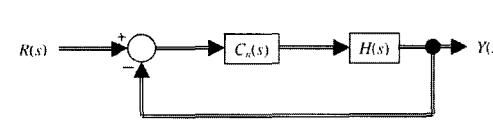

Fig. 3 Block diagram of a unity feedback contral system

In Eq. (14), a free parameter $Q(s)$ is given by

$$Q(s)=H^{-1}(s)H_m(s)\in RH_\infty$$
$$H_m(s)=\begin{bmatrix} H_{aam}(s) & 0 \\ 0 & H_{bbm}(s) \end{bmatrix} \quad (17)$$

where $H_m(s)$ is a desired closed loop transfer matrix and $H_{aam}(s)$, $H_{bbm}(s)$ are desired closed loop transfer functions for force and position control system respectively. A stabilizing controller $C_n(s)$ described in Eq. (14), after combining Eqs. (16) and (17), can be written as

$$C_n(s)=H^{-1}(s)H_m(s)(I-H_m(s))^{-1} \quad (18)$$

and closed loop transfer matrix of the unity feedback control system using the $C_n(s)$ becomes

$$H_0(s)=Y(s)R^{-1}(s)=H_m(s) \quad (19)$$

From Eq. (19), it can be known that using the controller given by Eq. (18), there is no interaction between inputs and outputs, therefore, changes in $F_r(s)$ affect only $F(s)$ and changes in $x_r(s)$ affect only $x(s)$.

4.2 Disturbance observer design

Non-interaction controller may be brought about position and force control error owing to the modeling error. In this section, the disturbance observer using $H_m(s)$ as an internal model is designed to compensate a modeling error and track a reference input more accurately. Fig. 4 shows the block diagram of the control system with the disturbance observer consisting of $J(s)$ and $H_m^{-1}(s)$.

In Fig. 4, $K(s)$ is a prefilter matrix to adjust reference input tracking performance, $d(s)$ is a disturbance representing modeling error of $H_0(s)$, $J(s)$ is a stabilizing filter matrix and $d_o(s)$ is an output of disturbance observer. Transfer matrices from $d(s)$ to $d_o(s)$ and $Y(s)$ are given by

$$d_o(s)d^{-1}(s)=[I-J(s)+J(s)H_m^{-1}(s)H_0(s)]^{-1}[J(s)H_m^{-1}(s)H_0(s)] \quad (20)$$

$$Y(s)d^{-1}(s)=[I-J(s)+J(s)H_m^{-1}(s)H_0(s)]^{-1}[H_0(s)(I-J(s))] \quad (21)$$

From Eqs. (20) and (21), if $\|J(s)\|=I$ then $d_o(s)=d(s)$ and $Y(s)=0$, therefore, it can be known that the disturbance observer estimate and compensate the modeling error within a frequency band of $\|J(s)\|=I$.

Fig. 4 can be transformed into Fig. 5 equivalently.

In Fig. 5, all realizable stabilizing controllers $C_1(s)$ and $C_2(s)$ derived from Youla parametrization are given by

$$C_1(s)=K(s)(\tilde{Z}_{H0}(s)-N_{H0}(s)Q_0(s))^{-1}$$
$$C_2(s)=\Omega(H_0(s))=(\tilde{W}_{H0}(s)+D_{H0}(s)Q_0(s))(\tilde{Z}_{H0}(s)-N_{H0}(s)Q_0(s))^{-1} \quad (22)$$

where $D_{H0}(s)$ and $N_{H0}(s)$ are the denominator and numerator of right coprime fraction of $H_m(s)$ and $\tilde{W}_{H0}(s)$, $\tilde{Z}_{H0}$ are matrices that satisfy the Bezout identity described in Eq. (23).

$$\tilde{N}_{H0}(s)\tilde{W}_{H0}(s)+\tilde{D}_{H0}(s)\tilde{Z}_{H0}(s)=I \quad (23)$$

where $\tilde{D}_{H0}$ and $\tilde{H}_{H0}(s)$ are denominator and numerator of left coprime fraction of $H_m(s)$. One of matrices satisfying Eq. (23) can be obtained as follows.

$$H_m(s)\in RH_\infty,\ N_{H0}(s)=\tilde{N}_{H0}(s)=H_m(s)$$
$$D_{H0}(s)=\tilde{D}_{H0}(s)=I,\ \tilde{W}_{H0}(s)=0,\ \tilde{Z}_{H0}(s)=I \quad (24)$$

In Eq. (22), a prefilter $K(s)$ and a free parameter $Q_0(s)$ are given by

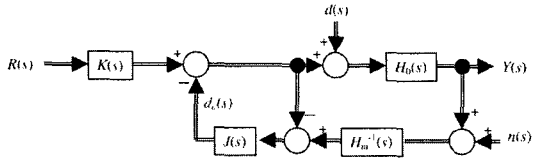

Fig. 4 Block diagram of the control system with a disturbance observer

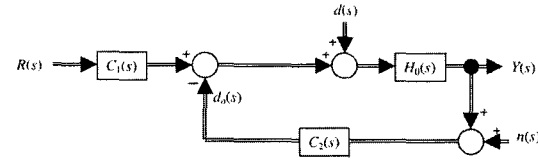

Fig. 5 Equivalent system of the control system described in Fig. 4

$$K(s)=H_m^{-1}(s)H_{YR}(s)\in RH_\infty$$
$$H_{YR}(s)=\begin{bmatrix}H_a(s) & 0\\ 0 & H_b(s)\end{bmatrix} \tag{25}$$

$$Q_0(s)=H_m^{-1}(s)J(s)\in RH_\infty$$
$$J(s)=\begin{bmatrix}J_a(s) & 0\\ 0 & J_b(s)\end{bmatrix} \tag{26}$$

where $H_{YR}(s)$ is the desired closed loop transfer matrix from $R(s)$ to $Y(s)$ in Fig. 4 and 5 and $J(s)$ is a stabilizing filter matrix.

Eq. (22), after combining Eqs. (24) and (26), can be written as

$$C_1(s)=K(s)(I-J(s))^{-1}$$
$$C_2(s)=H_m^{-1}(s)J(s)(I-J(s))^{-1} \tag{27}$$

4.3 Selecting the controller parameters

According to the conditions of Eqs. (17) and (26), $H_m(s)$ and $J(s)$ can be selected as follows.

$$H_{aam}(s)=\frac{\beta}{s+\beta}=\frac{H_{aamn}(s)}{H_{aamd}(s)}$$
$$\beta=K_{PF}\eta k_{qa}(A_1+A_2),\ K_{PF}=0.0125\ [\mathrm{V/N}] \tag{28}$$
$$H_{bbm}(s)=\frac{\alpha}{(s+\sqrt[3]{\alpha})^3}=\frac{H_{bbmn}(s)}{H_{bbmd}(s)}$$
$$\alpha=K_{PX}\eta k_{qb}(A_1+A_2),\ K_{px}=200\ [\mathrm{V/m}]$$

$$J_a(s)=\frac{3\beta}{s+3\beta},\ J_b(s)=\frac{3\alpha}{(s+\sqrt[3]{3\alpha})^3} \tag{29}$$

where K_{PF}, K_{PX} are control gains to specify the internal model $H_m(s)$.

In order to have a zero acceleration error and track asymptotically a reference input, $H_a(s)$ and $H_b(s)$ in Eq. (25) must be BIBO stable and has the following properties (Chen, 1999).

$$H_a(0)=H_b(0)=1$$
$$\dot{H}_a(0)=\dot{H}_b(0)=0 \tag{30}$$
$$\ddot{H}_a(0)=\ddot{H}_b(0)=0$$

Using a low-pass filter $C_f(s)$ and Eq. (28), the $H_{YR}(s)$ satisfying the conditions in Eqs. (25) and (30) can be selected as follows.

Table 1 Physical parameters of the pneumatic cylinder driving apparatus

A_1 [m^2]	1.26×10^{-3}	M [kg]	1.0
A_2 [m^2]	1.14×10^{-3}	P_{10} [Pa]	3.5×10^5
B [N/(m/s)]	223	P_{20} [Pa]	3.8×10^5
k_{p0} [(kg/s)/Pa]	3.09×10^{-9}	R [J/(kg·K)]	287
k_{qa} [(kg/s)/V]	1.95×10^{-3}	T_{atm} [K]	293
k_{qb} [(kg/s)/V]	1.44×10^{-3}	V_0 [m^3]	2.8×10^{-4}
L [m]	0.3	κ	1.4

$$C_f(s)=\frac{40^2}{(s+40)^2}=\frac{C_{fn}(s)}{C_{fd}(s)}\in RH_\infty$$
$$H_{aamd}(s)C_{fd}(s)=s^3+h_2s^2+h_1s+h_0$$
$$H_a(s)=\frac{h_2s^2+h_1s+h_0}{s^3+h_2s^2+h_1s+h_0} \tag{31}$$
$$H_{bbmd}(s)C_{fd}(s)=s^5+g_4s^4+g_3s^3+g_2s^2+g_1s+g_0$$
$$H_b(s)=\frac{g_2s^2+g_1s+g_0}{s^5+g_4s^4+g_3s^3+g_2s^2+g_1s+g_0}$$

Table 1 shows physical parameters of the driving apparatus.

5. Experimental Results and Discussions

Figures 7~10 show the experimental results with the various reference inputs. In Figs. 7~10, x_0 and F_0, initial value of position and force, are set to 0 [N] and 0.143 [m] respectively and, a proportional controller with the K_{PF} and K_{PX} was used as a reference control algorithm in order to verify the validity of the proposed control method. Fig. 6 shows the block diagram of the control system with the proportional controller.

In Figs. 7~10, e_x and e_f are the position and force control errors.

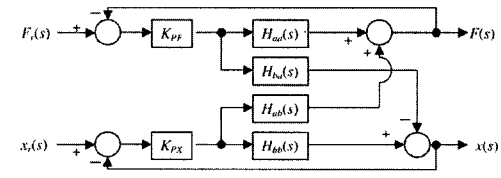

Fig. 6 Block diagram of the control system with a proportional controller

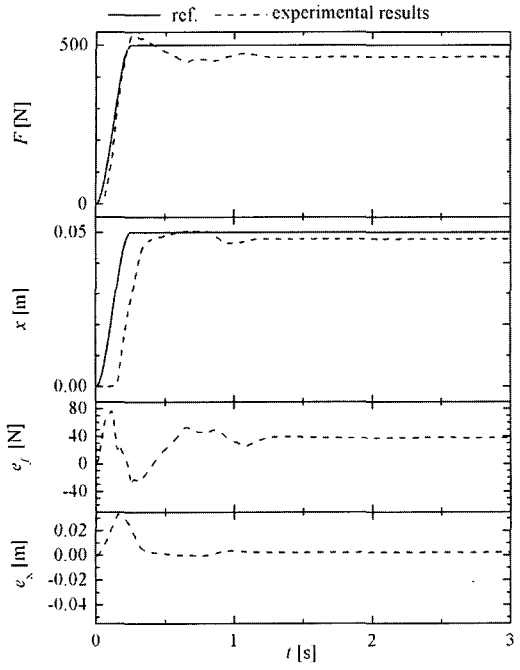

(a) Step width of F_r : 500 [N], x_r : 0.05 [m]

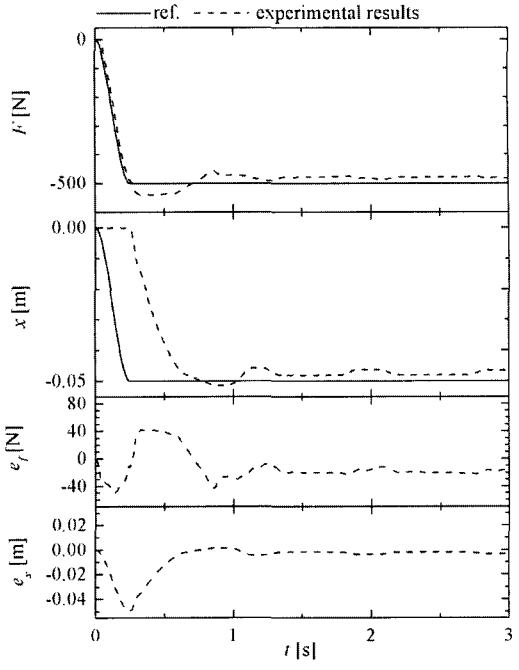

(b) Step width of F_r : −500 [N], x_r : −0.05 [m]

Fig. 7 Trajectory tracking control results with the proportional controller in case that the reference inputs of position and force are step inputs

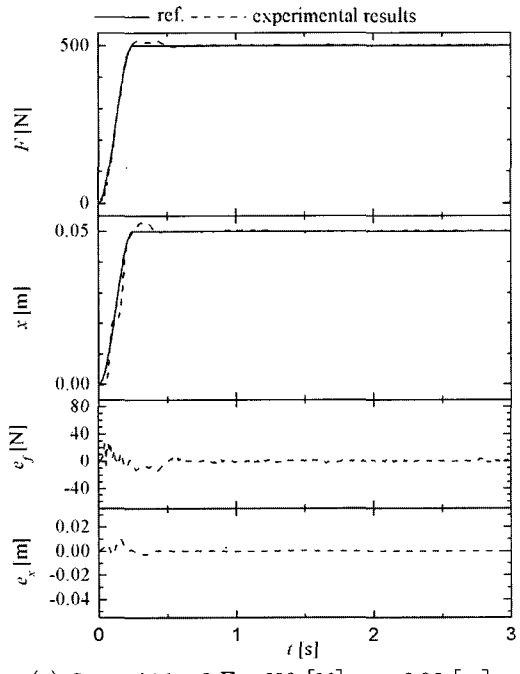

(a) Step width of F_r : 500 [N], x_r : 0.05 [m]

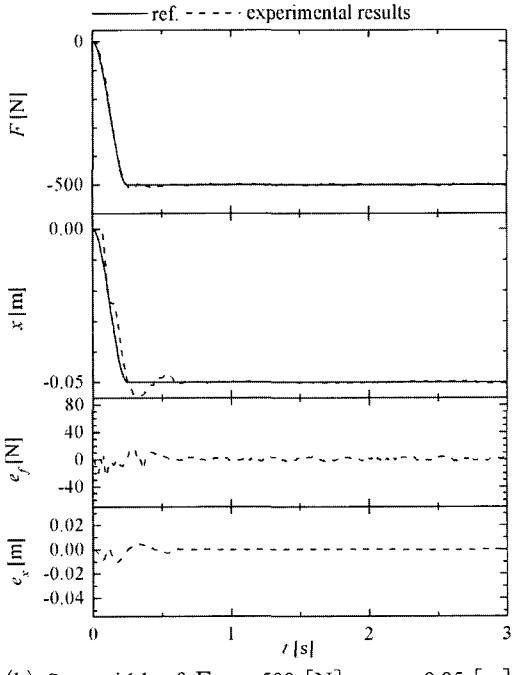

(b) Step width of F_r : −500 [N], x_r : −0.05 [m]

Fig. 8 Trajectory tracking control results with the proposed controller in case that the reference inputs of position and force are step inputs

Figures 7~8 show the experimental results in case that the reference inputs of position and force are step inputs. In Figs 7~8, solid lines are reference inputs and dash lines are experimental results. In Fig. 7, it can be observed that transient response of position and force trajectory with the proportional controller is changed by the variation of reference inputs, slack vibrations are shown in the vicinity of the steady state and a serious error occurs in the transient response and steady state response. In Fig. 8, it is clear that transient response of position and force trajectory with the proposed controller is not changed by the variation of reference inputs and, control errors with the proposed controller are materially reduced in the transient state and steady state where the mean value of e_x is -0.021 [mm] and e_f is 0.093 [N], and the standard deviation of e_x is 0.2 [mm] and e_f is 2.3 [N].

Figure 9 shows the results in case that the reference inputs of position and force are step input and sinusoidal input respectively. (a) shows the results when reference input of position was set to a step input and reference input of force was set to a sinusoidal input. It can be known that the results using proposed controller show good tracking performance for the reference input of force and, a little vibration was shown in the position response when the direction of force response was changed but the vibration was disappeared with course of time. (b) shows the results when reference inputs of position and force were set to a sinusoidal input and a step input respectively. It can be known that the control results with the proposed controller tracks given reference inputs well.

Figure 10 shows the results in case that the reference inputs of position and force are sinusoidal inputs. (a) shows the results when reference inputs of position and force were set to sinusoidal inputs having the same frequency. (b) shows the results when reference inputs of position and

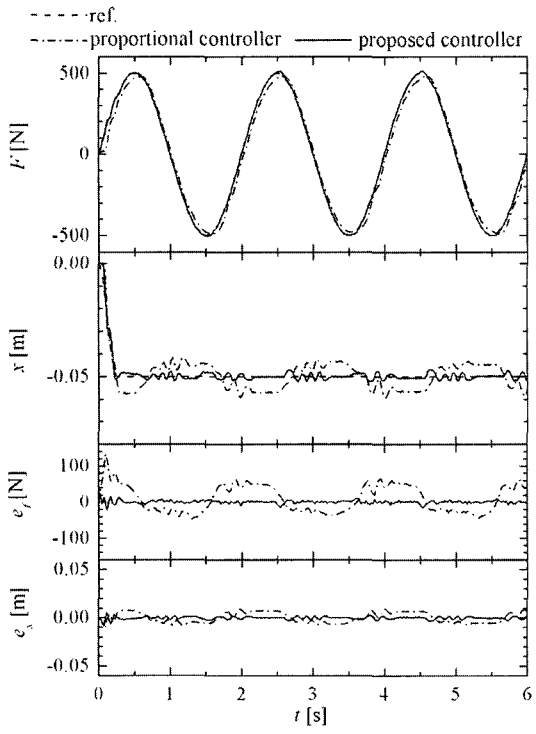

(a) F_r : sinusoidal input, x_r : step input

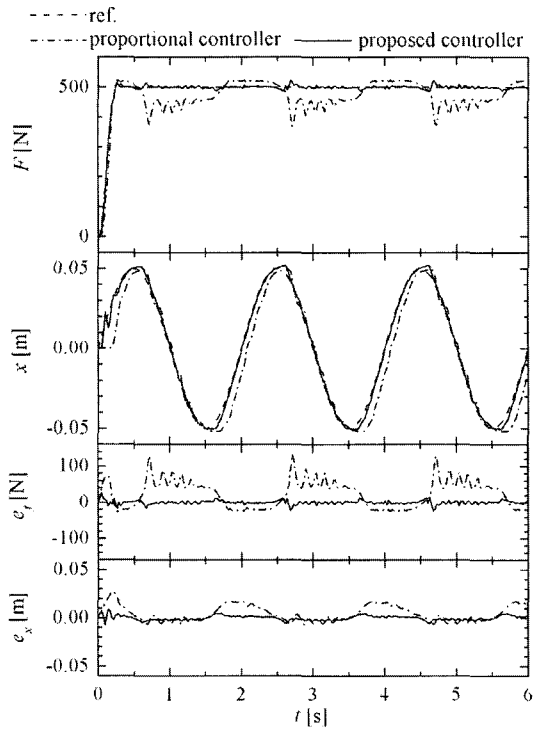

(b) F_r : step input, x_r : sinusoidal input

Fig. 9 Trajectory tracking control results in case that the reference inputs of position and force are step input and sinusoidal input respectively

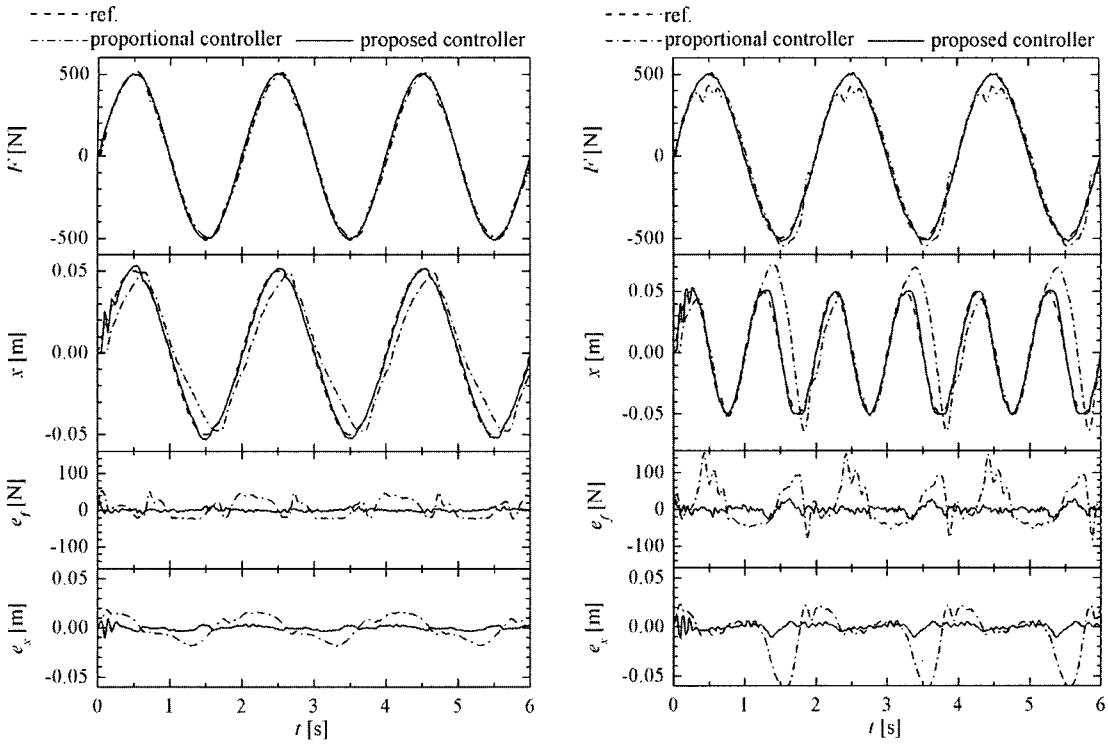

(a) Frequency of F_r : 0.5 [Hz], x_r : 0.5 [Hz]

(b) Frequency of F_r : 0.5 [Hz], x_r : 1.0 [Hz]

Fig. 10 Trajectory tracking control results in case that the reference inputs of position and force are sinusoidal inputs

force were set to sinusoidal inputs having the different frequency. It shows that the results with the proportional controller cannot track the given reference inputs but the results with the proposed controller track given reference inputs well.

6. Concluding Remarks

In this paper, a position and force simultaneous trajectory tracking control algorithm for the pneumatic cylinder driving apparatus is proposed. The control algorithm is derived from the Youla parametrization to insure stability of the control system. It is composed of the non-interaction controller eliminating an interaction between position and force control system based on the linear model of the driving apparatus, and the disturbance observer compensating the modeling errors and tracking the reference inputs more accurately. The experimental results show that the pneumatic cylinder driving apparatus with the proposed control algorithm has good tracking performance for the various reference inputs of position and force.

Acknowledgments

This work was supported by the Brain Korea 21 Project in 2005.

References

Chen, C. T., 1999, "Linear System Theory and Design. 3rd edition," *Oxford university press*, pp. 275~277.

Desoer, C. A., 1980, "Feedback System Design ; The Fractional Representation Approach to Analysis and Synthesis," *IEEE Trans. Automat. Control*, AC-25, No. 3, pp. 399~412.

Johira, T., 1997, "Pneumatic Servo System," *Transactions of the Japan Hydraulics and Pneumatics Society*, Vol. 28, No. 7, pp. 748~752.

Merritt, H. E., 1967, "Hydraulic Control Systems," *John Wiley & Sons, Inc.*, pp. 135.

McGuirk, D. P., Pingdong, W. and Xiao, X., 1998, "Fluid Power in the world," *Journal of the Japan Fluid Power System Society*, Vol. 29, No. 3, pp. 212~243.

Noritugu, T.,1993, "Control Characteristics of Pneumatic Cylinder," *Journal of the Japan Fluid Power System Society*, Vol. 24, No. 7, pp. 775~780.

Umeno, T. and Hori, Y., 1989, "Design of Robust Servo systems Based on the Parametrization of Two Degrees of Freedom Control Systems," *T. IEE Japan*, Vol. 109-D, No. 11, pp. 825~832.

Yamafuzi, K. and Fukushima, T., 1998, "Simultaneous Control of Vertical Position and Force of a Pneumatic Cylinder," *Transactions of the Japan Hydraulics and Pneumatics Society*, Vol. 19, No. 3, pp. 226~233.